Spatial Channel Characteristics for Macro- and Microcellular BS Installations

Klaus Hugl[1], Kimmo Kalliola[2], Juha Laurila[2]

[1]Institut für Nachrichtentechnik und Hochfrequenztechnik (INTHF)
Technische Universität Wien, Vienna, Austria
[2]Nokia Research Center, Helsinki, Finland
Klaus.Hugl@mobile.nt.tuwien.ac.at

Abstract: *We investigate the different dominant propagation mechanisms in an urban macro- and microcellular base station (BS) installation with a special focus on the application of smart antennas by means of adaptive antenna array measurements. We demonstrate that the congruence of the geometrical mobile station (MS) position and the dominant direction of arrival is only fulfilled for macrocellular BS installations. In microcells the propagation situation is different. There, street canyons play a significant role in mobile radio propagation in contrast to the macrocellular case, where over rooftop propagation prevails. This behavior has to be taken into account in system level simulations of adaptive antenna BS systems. Moreover, the different dominant propagation phenomena will strongly effect adaptive antenna operation for varying BS antenna heights.*

1. Introduction

The utilization of adaptive antennas in cellular mobile communication systems has raised significant interest in recent years [1]. Adaptive antennas applied at the BS are expected to boost the link quality and improve the spectral efficiency and capacity of 2nd and 3rd generation wireless systems. Realistic spatial channel models are the basis for the design of enhanced transceiver structures, adaptive antenna algorithm development and the estimation of the possible capacity gain. Spatial channel measurements are required to allow realistic parameterization and to provide further input for channel modeling in general.

As a consequence a lot of effort was spent in recent years for spatial channel measurements to improve the understanding of mobile radio propagation. The performed measurement campaigns investigated the directional nature of the mobile radio channel either at the mobile station (MS) [2,3] or as seen from a BS antenna array [4,5]. We were especially interested in the difference of dominant propagation effects in urban macro- and microcells as seen from a BS antenna array. Therefore, we conducted spatial channel measurements at the BS with different BS antenna array heights using a vehicular transmitter. We extract the spatial channel characteristics separately for macrocellular and microcellular BS installations and compare them.

In the following sections, we first describe the channel sounder setup and the performed measurements. Moreover, we compare the extracted spatial channel characteristics of macrocellular and microcellular BS installations by statistical evaluations of all measurements and a single sample measurement route in detail. Finally, we shortly discuss the consequences on channel modeling and smart antenna system level simulations.

2. Measurement Description

The spatial channel sounding campaign described herein was conducted by Nokia Research Center (NRC) Helsinki in cooperation with INTHF in June 2001 in downtown Helsinki. For measurement purpose the NORPPA channel sounder built by Elektrobit AG was applied.

In the measurements, a vehicular transmitter mounted on the roof of a measurement van at a height of about 1.8m above ground level was used. The sounding signal was either transmitted using a vertically polarized monopole or a dummy handset attached to a phantom head. The measurements were instantaneously performed on an uplink (f_{UL}=1935MHz) and downlink carrier (f_{DL}=2125MHz) in the UMTS band. A modulated PN-sequence with length 127 and a chip-rate of 5MChips/s was applied as channel sounding signal. We performed dynamic drive measurements with a target speed of 40km/h in the center of Helsinki along different measurement routes. The dynamic drive measurements allow the spatial channel characterization for full BS sector coverage without the lack of limited statistics.

At the receiver/BS position an 8-column uniform linear array (ULA), each column consisting of 4 vertically polarized dipoles was applied. Each column of the physical array has a gain of 11dBi and 3dB-beamwidth of 120° in the horizontal (azimuthal) domain and 18° in the vertical plane. The inter-column distance was d=67mm corresponding to $0.432\lambda_{UL}$ and $0.475\lambda_{DL}$. The array was mechanically downtilted by 7° to maximize the sounding coverage.

The signals of the 8 antenna columns were collected using the fast RF switching technique [6]. In the receiver 4-times oversampling was applied resulting in a delay resolution of $\Delta\tau$=50ns. A single recorded array channel impulse response **h** has a dimension of 8 spatial samples (number of antenna columns) versus 508 delay samples

$$\mathbf{h} = \begin{bmatrix} h_1(0\cdot\Delta\tau) & \cdots & h_1(507\cdot\Delta\tau) \\ \vdots & & \vdots \\ h_8(0\cdot\Delta\tau) & \cdots & h_8(507\cdot\Delta\tau) \end{bmatrix}. \quad (1)$$

A measurement of a full array channel impulse response was performed every 3.6ms. Therefore, at least 3 channel snapshots per wavelength are available while the transmitter was moving along the measurement routes.

The antenna array receiver was placed on two different BS positions. For the macrocellular BS installation the array was placed on the roof of the Helsingin Energia building with an array orientation of 160° from map north. The microcellular BS installation was located less than 10m below the rooftop on a balcony of the Helsingin Energia building with the same array orientation. The photos of the receiver measurement setup for the macrocellular and microcellular BS installation are shown in Figure 1.

(a) (b)

Figure 1: The receiver setup for the macrocellular (a) and microcellular (b) BS installation at the Helsingin Energia building.

We measured in a dense urban environment with buildings having 6-7 storeys. For the macrocellular BS installation (on the rooftop of the Helsingin Energia building), the array is placed above the

rooftop level of the surrounding buildings. In the microcellular case we are approximately at or a little below the rooftop level of the buildings in the vicinity.

For the macrocellular and the microcellular BS installation the same drive routes were selected. Therefore, a direct comparison of the dominant propagation mechanisms depending on the BS antenna height is possible. Figure 2 shows a map indicating the array orientation and the performed drive routes in this 120° sector.

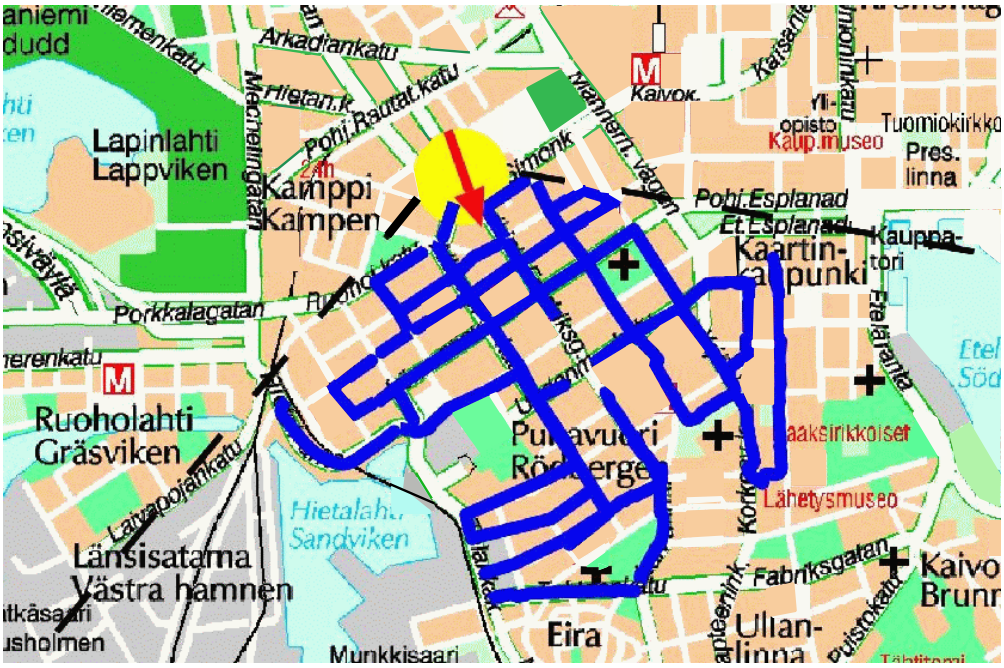

Figure 2: Map of the measurement scenario: The red arrow demonstrates broadside direction of the array. The blue lines illustrate the measurement routes for the macrocellular and microcellular BS installation. The black dashed lines indicate the sector borders assuming strict 120° sectorization.

We tried to measure full sector coverage and distributed the drive routes accordingly. In total, more than $5 \cdot 10^5$ complex array channel impulse responses along the drive routes of more than 20km for each of the BS installations were recorded. More details on the measurement setup and the propagation environment can be found in [7]. In the following section, we will investigate the directional nature of the mobile radio channel as seen from the BS for the above described BS installations only.

3. Measurement Data Evaluation and Results

Along the drive measurements, the GPS coordinates of the actual transmitter position were stored with time-tags. Therefore, it was possible to evaluate the geometrical angle between the transmitter position (LOS direction) and array broadside for each channel impulse response.

It is of interest to compare the geometrical angle given by the transmitter position with the dominant physical direction of arrival (DOA) of the impinging waves. We define the dominant DOA as the direction of maximum output power using the Bartlett beamformer [8]

$$\varphi_{dom} = \arg\max_{\varphi} \left\{ \sum_{n=0}^{507} \left| \mathbf{a}^H(\varphi) \cdot \mathbf{h}(n \cdot \Delta\tau) \right|^2 \right\}, \qquad (1)$$

where $\mathbf{a}(\varphi)$ and $\mathbf{h}(n \cdot \Delta\tau)$ denote the array steering vector of the ULA and the n-th delay sample of the recorded complex channel impulse response, respectively. The distribution of the deviation of

geometrical angle and dominant DOA for the macrocellular and microcellular BS installations are illustrated in Figure 3.

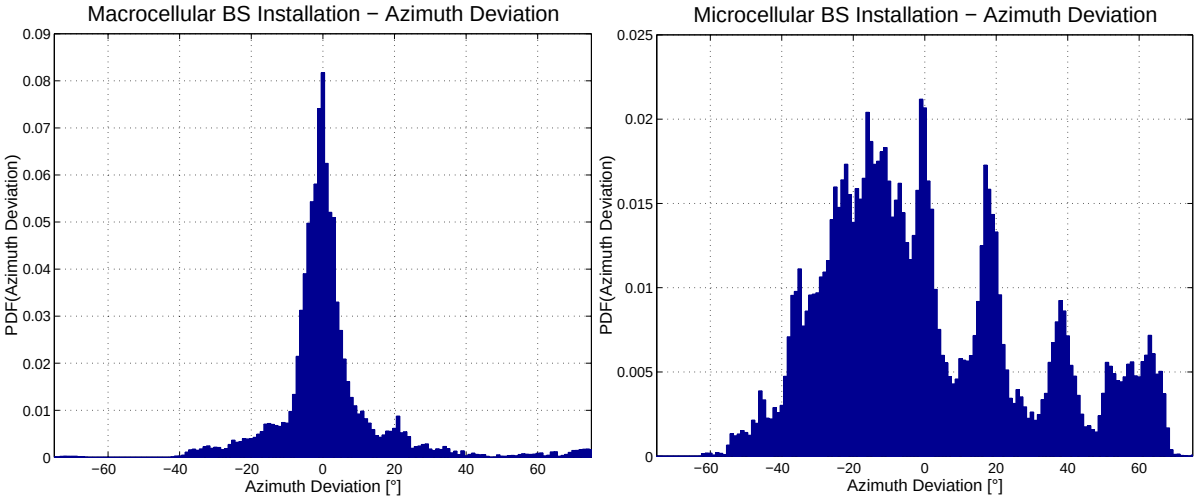

(a) (b)

Figure 3: Deviation between geometrical angle and the dominant direction of arrival for the macrocellular BS installation (a) and the microcellular case (b).

For the macrocellular installation in Fig. 3a, the dominant DOA shows a nice congruence with the geometrical angle. In most cases the waves propagate over the rooftop via the pseudo-LOS path from the transmitter to the receiver. The remaining deviation (the gaussian shape around 0 deviation) is beside other effects caused by the limited GPS accuracy in dense urban environments and the angular selective fading (shown in [9]).

For the microcellular installation less than 10m below the macrocellular installation the situation is totally different, as shown in Fig. 3b. Due to the lowered BS antenna height the waves propagating over the rooftop of the surrounding buildings have to be diffracted over the rooftops down to the BS antenna. Additionally, we have to keep in mind that the antenna array is tilted down by 7° to maximize the coverage area. Therefore, the antenna gain of the BS antenna array in the direction of the rooftop level is smaller for the microcellular BS installation. Thus, the signal contributions received by the adaptive antenna array from over the rooftop is not dominant any more. For the microcellular case the wave guiding in the streets directed towards the BS (cmp. Fig. 1) plays a significant role. The dominance of the wave guiding in the microcellular case can be easily identified by considering the distributions of the geometrical angle and the dominant DOA for all measurement routes, illustrated in Fig. 4a.

In the azimuth distribution there are two areas present where the DOAs do not correspond to the distribution of the geometrical angle. The first area is around –35° and belongs to the street canyon of Fredrikinkatu. The end of this street can be seen in the center of the picture of the macrocellular BS installation of Fig. 1a. The second dominant area is located in the range of 20° to 35°. This street canyon is the connection street towards Albertinkatu and Ruoholahdenkatu and can be seen in Fig. 1b. These two street canyon directions dominate the physical wave propagation for the microcellular BS installation. Similar spatial propagation behavior dominated by the street canyons was also recognized in [5].

To further improve the understanding of the differences in wave propagation for the macrocell and microcell, let us investigate the azimuth power spectrum (APS) along a single measurement route. We have chosen a sample route that nearly crosses the full sector from the left to the right as illustrated in Fig. 4b. In Fig. 4b the sample measurement route is marked with a white dashed arrow.

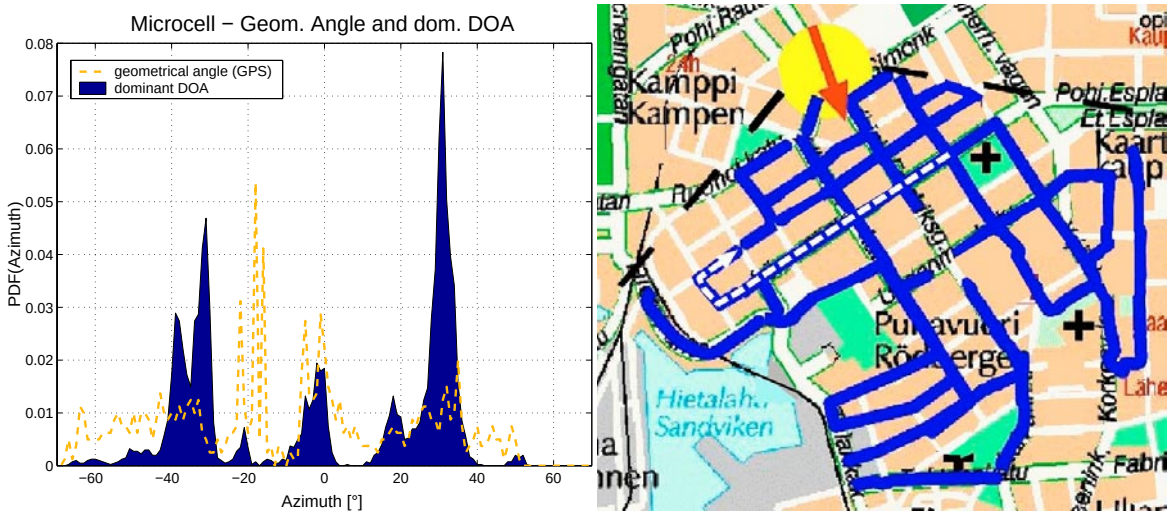

(a) (b)

Figure 4: Distribution of the geometrical angle and the dominant DOA for the microcellular BS installation (a). Map of the measurement sector including the sample measurement route (white dashed arrow) for the macrocellular and microcellular BS installation in (b).

For estimation purpose of the APS we use the least-squares power estimator (Capon´s beamformer or Minimum Variance Estimator [10])

$$P(\varphi) = \frac{1}{\mathbf{a}^H(\varphi) \cdot \mathbf{R}^{-1} \cdot \mathbf{a}(\varphi)} \tag{2}$$

applied on the spatial covariance matrix

$$\mathbf{R} = E_t\left\{\sum_{n=0}^{507} \mathbf{h}(n \cdot \Delta\tau) \cdot \mathbf{h}^H(n \cdot \Delta\tau)\right\}. \tag{3}$$

We average the channel snapshots collected within 1s for the expectation operation in (3) to get an estimate of the spatial covariance matrix. Moreover, we normalize the spatial covariance matrices to have unit total received power

$$\mathbf{R}_{norm} = \mathbf{R} / trace\{\mathbf{R}\} \tag{4}$$

in the estimation of the APS of Equ. (2). Therefore, the effect of changes in received signal power due to large scale fading is not visible and we only see the angular power distribution independent of the actual received signal power. The estimated azimuth power spectrum $P(\varphi)$ along the sample measurement route of Fig. 4b for the macrocellular and microcellular BS installation are shown in Fig. 5 and Fig. 6, respectively.

With the array installation on top of the Helsingin Energia building (macrocell, Fig. 5) the azimuth region where most power is received nicely follows the geometrical transmitter position. As an exception in the area of 80-100s there is a second angular cluster present, which does not correspond to the geometrical direction (street canyon towards Albertinkatu and Ruoholahdenkatu of Fig. 1b). However, overall there is a nice congruence of the geometrical azimuth angle and the dominant azimuthal areas where the signals impinge at the BS antenna array.

In contrast to these results, in the microcellular situation of Fig. 6 there is an angular clusterization defined by the street canyons visible. As the transmitter moves along Lönnrotinkatu (the first 100 seconds) the waves are first coupled through Fredrikinkatu towards the BS ($\varphi \approx -35°$). Later on, the coupling through Fredrikinkatu becomes less important and the strongest propagating waves have an azimuthal DOA of $\varphi \approx 25°$. In this case the wave guiding in the street canyon occurs through Albertinkatu or Ruoholahdenkatu towards the BS (compare the photo Fig 1b). At the end of this drive route the coupling towards these two streets is not any more so strong and the pseudo-LOS direction

with over rooftop propagation is also present in the microcellular case. This is because the signal would have to be guided through several different streets and diffracted around the corners before Albertinkatu or Ruoholahdenkatu would act as the final wave guide. This findings are well in line with the results presented in [11].

Of course the physical propagation effects are independent of the BS antenna height. But their relative importance in sense of received power of over the rooftop propagation and wave guiding in the street canyons is dependent on the BS antenna height in conjunction with the rooftop level and the street directions around the base station. The APS of the sample measurement route in Fig. 5 and Fig. 6 both indicate the wave guiding in the street canyon towards the BS at $\varphi \approx 25°$. For the macrocellular BS installation the signal power received from the pseudo-LOS direction over the rooftop is larger than from the street canyon. For the lower BS antenna installation the situation is vice versa. The relative importance of different propagation effects dependent on the BS antenna height has to be taken into account in the parameterization of spatial channel models.

Further evaluation results regarding the effect of the BS antenna height on path-loss and the delay characteristics of the mobile radio channel for this measurement campaign can be found in [7].

4. Consequences on Channel Modeling and System Level Simulations

The investigations strongly indicate that for a macrocell the dominant direction of arrival shows a nice congruence with the geometrical mobile station position. The propagation is strongly dominated by waves propagation over the rooftop of the surrounding buildings via the pseudo-LOS path. This is in line with the channel modeling assumption that local scattering around the mobile station occurs and the dominant direction of arrival is defined by the mobile station position. Moreover, most system level simulators of cellular mobile communication systems including smart antennas (e.g. [12,13]) are based on this assumption. As a consequence, the angular separability of the users defined by their azimuthal location automatically leads to the angular separability using an adaptive antenna array at the BS. Therefore, smart antennas applying beampointing can be used to decrease the co-channel interference and, as a consequence, to improve the system capacity [14].

In case of a microcellular BS installation, the dominant azimuthal regions are very much defined by the streets directed towards the BS. The signals of several users within the sector will propagate through the same street canyons also if they are not located in the same area. Therefore, other modeling approaches for system level simulators have to be developed to be able to estimate the system capacity increase of microcellular adaptive antenna BS installations below the rooftop level. A lot of system level simulations will have to be performed to find out in which way adaptive antennas can cope with the situation of the concentration of the spatial channel characteristics of several users to some azimuthal areas.

5. Conclusions

We have performed dynamic drive measurements in an urban environment. We compared the dominant angular behavior as seen from an adaptive antenna array using an urban macrocellular and microcellular base station installation. The investigations indicate that for macrocellular BS installations there is a nice congruence of the geometrical MS position and the dominant DOA. The physical wave propagation is dominated by over rooftop propagation via the pseudo-LOS path. For microcellular BS installation the situation is totally different. Wave guiding in street canyons plays a significant role and the dominant DOA is mainly defined by the orientation of the street canyons and not by the geometrical user position. Therefore, other angular modeling approaches than the geometrical user position have to be used in system level simulators to be able to realistically estimate the capacity improvement that multi-antenna BS systems can provide in microcells with the antenna array below the rooftop level.

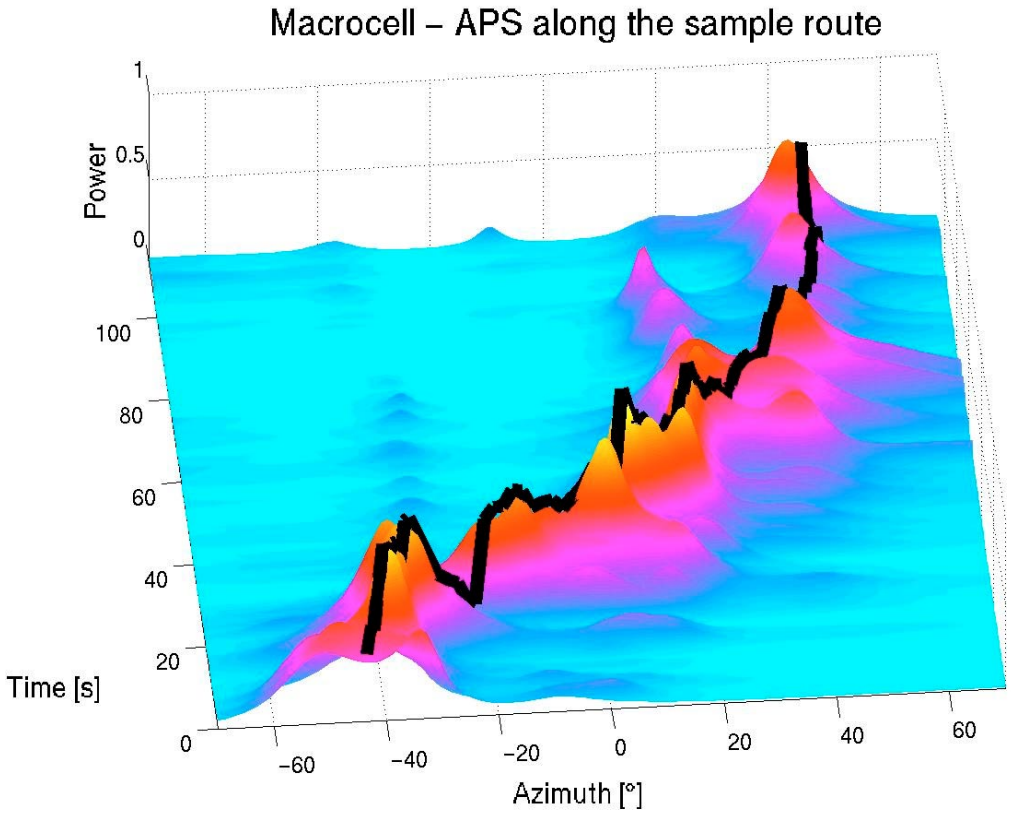

Figure 5: Azimuth power spectrum (APS) along the sample measurement route for the macrocellular BS installation. The black line along the APS illustrates the geometrical angle according to the transmitter position.

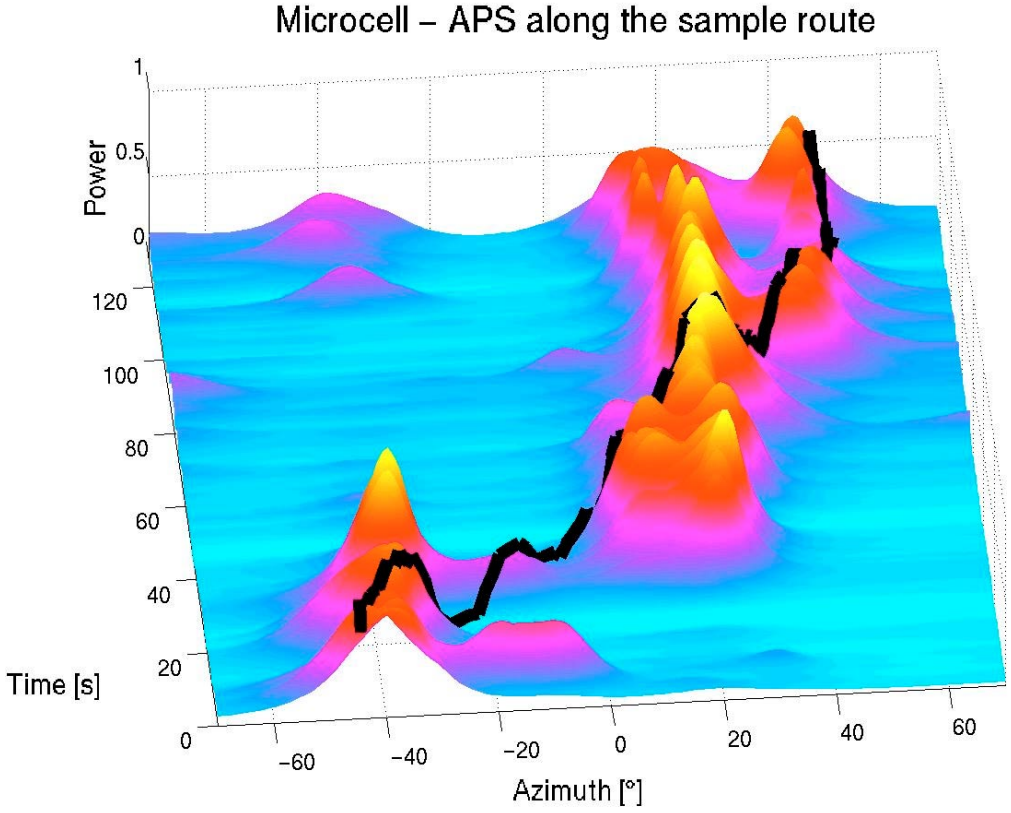

Figure 6: Azimuth power spectrum (APS) along the sample measurement route for the microcellular BS installation. The black line along the APS illustrates the geometrical angle according to the transmitter position.

Acknowledgments and Remarks

Special thanks to Sonera Corporation® for allowing to use their licensed UMTS band for channel sounding purpose. Please note that the views put forward in this paper are solely ours, and do not necessarily reflect the views of NOKIA Corporation®.

References

[1] A. J. Pauraj, C. B. Papadias, "*Space-Time Processing for Wireless Communications*", IEEE Signal Processing Magazine, No. 6, Vol. 14, pp. 49-83, November 1997.

[2] A. Kuchar, J.-P. Rossi, E. Bonek, "*Directional Macro-Cell Channel Characterization from Urban Measurements*", IEEE Transactions on Antennas and Propagation, Vol. 48, No. 2, pp. 137-146, February 2000.

[3] K. Kalliola, H. Laitinen, K. Sulonen, L. Vuokko and P. Vainikainen, "*Directional Radio Channel Measurements at Mobile Station in Different Radio Environments at 2.15 GHz*", Proc. EPMCC'2001, Vienna, Austria (2001).

[4] K. I. Pedersen, P. E. Mogensen and B. H. Fleury, "*Spatial Channel Characteristics in Outdoor Environments and their Impact on BS Antenna System Performance*", Proc. IEEE VTC'98, pp. 719-723, Ottawa, Canada (1998).

[5] J. Laurila, K. Kalliola, M. Toeltsch, K. Hugl, P. Vainikainen, E. Bonek, "*Wideband 3-D Characterization of Mobile Radio Channels in Urban Environment*", IEEE Transactions on Antennas and Propagation, February 2002.

[6] K. Kalliola and P. Vainikainen, "*Characterization System for Radio Channel of Adaptive Array Antennas*", Proc. IEEE PIMRC'97, pp. 95-99, Helsinki, Finland (1997).

[7] K. Hugl, "*Spatial Channel Characteristics for Adaptive Antenna Downlink Transmission*", Dissertation, 192p., Institut für Nachrichtentechnik und Hochfrequenztechnik, Technische Universität Wien, January 2002.
available at http://www.nt.tuwien.ac.at/mobile/theses_finished/

[8] M. Bartlett, "*Smoothing Peridiograms from Time Series with Continuous Spectra*", Nature, No. 161, 1948.

[9] J. Bach Andersen, K.I. Pedersen, "*Angle-of-arrival statistics for low angular resolution*", Proc. EPMCC'2001, Vienna, Austria (2001).

[10] J. Capon, R. J. Greenfield, R. J. Kolker, "*Multidimensional Maximum-Likelihood Processing of a Large Aperture Seismic Array*", Proceedings of IEEE, Vol. 55, pp. 192--211, February 1967.

[11] J. Li, J.-F. Wagen, E. Lachat, "*Propagation over the Rooftop and in the Horizontal Plane for Small and Micro-cell Coverage Predictions*", Proc. IEEE VTC´97, pp. 1123-1127, Phoenix, Arizona, USA (1997).

[12] T. Neubauer, E. Bonek, "*Smart-Antenna Space-Time UMTS Uplink Processing for System Capacity Enhancement*", Annales des Télécommunications, Special Issue on UMTS, Vol. 56, pp. 306--316, May-June 2001.

[13] M. Haardt, C. Mecklenbräuker, M. Vollmer, P. Slanina, "*Smart Antennas for UTRA TDD*", European Transactions on Telecommunications (ETT), Special Issue on Smart Antennas, Vol. 12, No. 5, pp. 393-406, September/October 2001.

[14] A. F. Naguib, A. Paulraj, T. Kailath, "*Capacity Improvement with Base-Station Antenna Arrays in Cellular CDMA*", IEEE Transactions on Vehicular Technology, Vol. 43, No.3, pp. 691-698, August 1994.